

# The Crystal Structure Analysis by the Subsidiary Maxima of the Electron Diffraction Pattern\*

Natsu UYEDA\*\*

(Suito Laboratory)

*Received December 4, 1957*

A new method for determining the crystal structure is presented, which is entirely based on the measurement of linear components of the electron diffraction pattern instead of the intensity of the diffraction as ordinary procedure used so far for structure analysis in X-ray and electron diffraction methods.

The linear components of the diffraction pattern used here were those of the subsidiary maxima of diffraction spots. According to the dynamical theory of the electron diffraction, the displacement of the subsidiary maximum from the main diffraction spot gives the Fourier potential  $V_{hkl}$  of the periodic field of the crystal lattice, which in turn gives some information about the structure factor of the crystal itself. A practical method for analysis of subsidiary diffraction spots to calculate the Fourier potential was developed. A result of the application of this method to determine the unknown parameter of cadmium bromide was also presented as an example of one parameter case.

## I. INTRODUCTION

In X-ray crystallography, almost all of the works so far made for determining the parameter, the position of each atom in the unit cell, depended on the analysis of the intensity of the diffracted X-ray beam by the crystal. When the electron diffraction method was used, the situation was the same. Though such procedure depending on the intensity measurement are the most regular and orthodox ones, the intensity measurement itself demands many techniques of high grades and serious precaution. The principle of the method reported here, for determining the crystal parameter, depends only on the measurement of geometrical quantities such as the linear distance and angular relationship of reflections described on the electron diffraction pattern and has a great advantage because the precise measurement of such linear components is much easier than the intensity measurement.

The linear components of the diffraction pattern used here are those of the fine structure of diffraction spots accompanied by subsidiary maxima. The theoretical principle of this method is mainly based on the dynamical theory of electron diffraction which was developed by Bethe<sup>1)</sup>, MacGillavry<sup>2)</sup>, and Kato and Uyeda<sup>3)</sup>.

On the other hand, recent advance in the electron optics made it possible to

---

\* Read at the Symposium for the Crystal Structure Analysis by the Electron Diffraction Method, held by the Physical Society of Japan, in Osaka on November 25th, 1956.

\*\* 植田 夏

increase the resolving power of the electron diffraction pattern by the use of electron lenses in a diffraction unit and to describe such fine structures as subsidiary maxima which appear in the elongated intensity regions of reciprocal lattice points for thin lamellar crystals, split diffraction spots caused by the refraction effect of micro-crystals of various shapes, and so on. Recently, Cowely, Goodman and Rees<sup>4)</sup> also reported a similar method to draw a section of the potential map of the micro-crystal of magnesium oxide using the Fourier potentials calculated from the linear component of the split spot groups of the electron diffraction pattern.

The small intervals of the subsidiary maxima also give some information about the Fourier potential  $V_{hkl}$  of the periodic lattice structure of the crystal, and, moreover, the  $V_{hkl}$  is closely related to the structure factor which give us the final information about the lattice parameter itself.

The works relating to the analysis of subsidiary diffraction spots were made by Hashimoto<sup>5)</sup> with a molybdenum oxide crystal and by Uyeda et al.<sup>6)</sup> with the crystal of molybdenum sulfide, both for the verification of the dynamical theory itself, and the results proved the good coincidence between the theoretically and experimentally obtained values of the Fourier potential for the crystal of a known lattice structure. A similar work was also reported by the author<sup>7)</sup> on an application to calculate the thickness of the specially prepared lamellar crystals of colloidal gold.

A report is hereby made on the results of the application of this method to determine the position of the halogen atoms in the hexagonally close-packed layer lattice with the lamellar micro-crystal of cadmium bromide, as an example of the one parameter case.

## II. THEORETICAL

According to the dynamical theory of electron diffraction, the interference function along the normal direction to a principal habit surface of the crystal is given, in place of the kinematical one, by a slightly modified form as,

$$\sin^2 \pi M h_L / (\pi h_L)^2, \quad (1)$$

where  $M$  is the number of atomic lattice normal to the direction along which Eq. 1. is defined. The dynamical modification is made on the quantity  $h_L$  in the form as

$$h_L = \sqrt{h^2 + (2d_N q)^2} \quad (2)$$

where  $h$  is the parameter in the reciprocal lattice along the direction normal to the principal habit surface, and  $d_N$  is the lattice spacing of the net plane normal to the same direction. Furthermore,  $q$  is given by

$$2d_N V_{hkl} / \lambda E \sqrt{\cos \theta_1 \cdot \cos \theta_2}, \quad (3)$$

where  $V_{hkl}$ , ascribed to the spot of  $(hkl)$  reflection, is the Fourier potential of the periodic field in the crystal, and  $\theta_1$  and  $\theta_2$  respectively correspond to the angles contained between the normal to the crystal habit surface and the direction of incident and diffracted electron beam, whose wave length is equal to  $\lambda$  under the

accelerating voltage  $E$ . In such a modified form, the periodic function expressed in Eq. 1. has its maxima at the point where the parameter  $h_n$  is given by

$$h_n^2 = \left( \frac{2n+1}{2M} \right)^2 - \left( \frac{d_N V_{h,n,l}}{\lambda E \sqrt{\cos \theta_1 \cos \theta_2}} \right)^2 \quad (4)$$

where  $n$  is ordinal number for the subsidiary maxima and takes positive integer.

When the crystal takes layered structure, whose lattice spacing  $d_N$ , and has a lamellar crystal habit, whose flat surface is parallel to the layer, thickness  $D$  of the crystal is given by

$$D = M \cdot d_N \quad (5)$$

When the crystal is thin and  $M$  is small, the interval as well as the height of the subsidiary maxima become larger than those of the thicker crystal, as revealed by the Eq. 1; and this fact explains the elongation of the intensity region of the reciprocal lattice point in the direction normal to the habit surface. It is the advantage of the electron diffraction method, that, owing to the great interfering ability of the electron beam with the atoms, the sufficient intensity can be obtained for the diffracted beam even when the  $M$ , which is the number of the diffraction lattices, is small. This results in the complete separation of the subsidiary maxima in the final diffraction pattern, coupled with the increase in the resolving power of the electron diffraction apparatus. These subsidiary maxima can be realized on the diffraction pattern by artificial rotation or fortuitous bending of the lamellar crystal as shown in Fig. 1, where the latter case is illustrated.

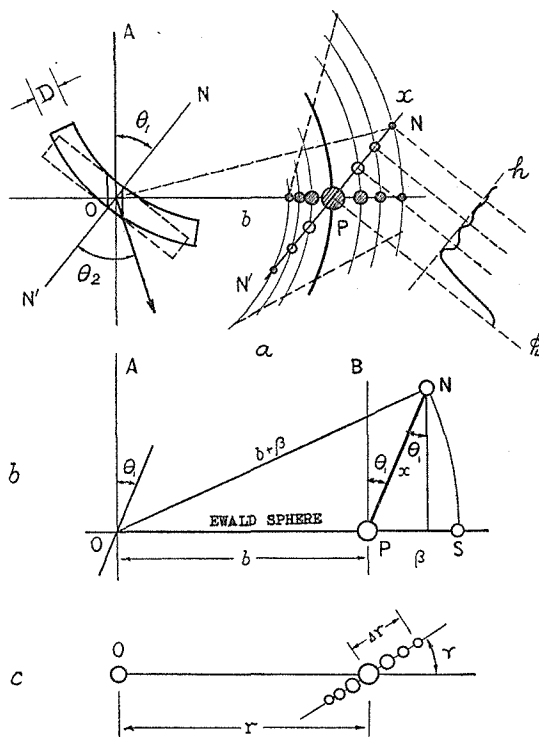


Fig. 1. Schematic illustration of the analysis of subsidiary maxima of elongated diffraction spots.

For the interpretation and the analysis of the electron diffraction pattern, it is convenient to consider the relationship between the reciprocal lattice and the Ewald sphere, as the intersection of the two reveals the diffraction pattern itself. In Fig. 1 (a), O and P are respectively the origin and the reciprocal lattice point, whose index is  $(hkl)$  and to which the principal maximum of Eq. 1 is ascribed. The direction NN' is parallel to the normal of the flaky habit surface of the lamellar crystal, which is superimposed as a section at the origin. On the line NN', the small blank circles, ranking symmetrically on both sides of the principal maximum correspond to the position of subsidiary maxima of the interference function, which is shown schematically by the curve in the space.

When the crystal is rotated or bent around an axis perpendicular to the plane containing the three points, O, P and the dispersion point A, the resultant rotation of the whole reciprocal lattice around the same axis at the origin causes the subsidiary diffraction points to describe concentric circles, as shown by the arcs in the figure. When the Ewald sphere cuts through the point  $(hkl)$ , the section of these circular loci appears as the subsidiary maxima of the diffraction spots of the "elongation". When the simplest case is dealt with, where the normal NN' is also contained in the OPA plane, the relationship between the intervals of the subsidiary diffraction spots and those of reciprocal lattice can be revealed. Let  $\Delta\theta_n$  be the angular displacement contained between the principal spot and each  $n$ -th subsidiary one, which appears on the outer side on the main spot in the diffraction pattern, then the relationship between  $\Delta\theta_n$  and  $h_n$ , the displacement of the  $n$ -th subsidiary maxima from the main one in the NN' direction, is given by

$$h_n = d_N \left\{ \sqrt{\frac{\sin^2 \theta_1}{d^2} + \frac{2\Delta\theta_n}{\lambda d} + \frac{(\Delta\theta_n)^2}{\lambda^2}} - \frac{\sin \theta_1}{d} \right\}, \quad (6)$$

where  $d$  is the interplanar spacing of the  $(hkl)$  plane,  $\theta_1$  is the angle between the normal of the crystal and the incident electron beam. The procedure of deriving this equation is obvious from Fig. 1 (b), because the following relation can easily be brought about;  $(b + \beta)^2 = x^2 \cos^2 \theta_1 + (b + x \sin \theta_1)^2$  where  $b$ ,  $\beta$  and  $x$  represent such quantities as  $1/d$ ,  $\Delta\theta_n/\lambda$  and  $h_n/d_N$  respectively, which are characteristic of the reciprocal lattice. In the above case, the series of subsidiary diffraction spots rank on a line in the radius direction. But, in general, they often deviate from the same direction, because the rotation axis is not always perpendicular to the  $\Delta OP$  plane when fortuitous warping of the crystal is expected instead of the artificial rotation. In such a case, a generalized form of Eq. 6 must be used, which can be represented as:

$$h_n = d_N \left\{ \sqrt{\frac{\sin^2 \theta_1 \cos^2(\gamma + \sigma)}{d^2} + \frac{2\Delta\theta_n \cos \gamma}{\lambda d} + \frac{\Delta\theta_n^2}{\lambda^2}} - \frac{\sin \theta_1 \cos(\gamma + \sigma)}{d} \right\}. \quad (7)$$

Where  $\gamma$  and  $\sigma$  are the angles between the radius direction passing through the main point and ranking direction of the subsidiary diffraction spots and also the projection of the normal through the main point is taken on the Ewald sphere respectively. (See Fig. 6 in the Appendix.) When the rotation axis is contained in the Ewald sphere which is approximated by a plane in an ordinary manner,  $\sigma$  becomes zero, and Eq. 7 can be reduced to the next form:

Crystal Structure Analysis by Subsidiary Diffraction Maxima

$$h_n = d_N \left[ \left\{ \frac{\sin^2 \theta_1 \cdot \cos^2 \gamma}{d^2} + \frac{2\Delta\theta_n \cos \gamma}{\lambda d} + \frac{\Delta\theta_n^2}{\lambda^2} \right\}^{\frac{1}{2}} - \frac{\sin \theta_1 \cos \gamma}{d} \right] \quad (8)$$

The same result can be obtained by replacing  $d$  in Eq. 6 by  $d/\cos \gamma$ . In practice, following equation is most useful which can be given by the replacement of  $\Delta\theta_n/\lambda$  with  $\Delta r_n/(rd)$  where  $\Delta r_n$  is the lineae displacement of  $n$ -th subsidiary diffraction spot from the main one whose radius is given by  $r$ :

$$h_n = \frac{d_N}{d} \left\{ \left[ \sin^2 \theta_1 \cos^2 (\gamma + \sigma) + 2 \frac{\Delta r_n}{r} \cos \gamma + \left( \frac{\Delta r_n}{r} \right)^2 \right]^{\frac{1}{2}} - \sin \theta_1 \cos (\gamma + \sigma) \right\} \quad (9)$$

Furthermone, when subsidiary diffraction spots rank on the radius direction through the main spot, Eq. 8 completely accords with Eq. 6, as in such a case  $\gamma$  vanishes. The procedure to derive Eq. 7 is shown in the Appendix.

On the other hand,  $V_{hkl}$  is related to the structure factor through the following equation:

$$V_{hkl} = \frac{ed^2}{\pi V} \cdot F_{hkl} = \frac{ed^2}{\pi V} \sum (Z-f) e^{-2\pi i (x, y, z)} \quad (10)$$

where  $V$  is the volume of the unit cell. The structure factor  $F_{hkl}$  of the crystal corresponds to the term under the summation which must be carried out all over the unit cell. When the space group of the crystal is determined from the diffraction data by taking the index of each reflection into consideration, then the structure factor can be derived though it contains the unknown parameters, which in turn can be solved by several  $V_{hkl}$  values through Eqs. 8-10.

As an example of the one parameter case, the hexagonal crystal of  $R\bar{X}_2$  type whose space group is  $R\bar{3}m$  was dealt with in the present work. The crystal

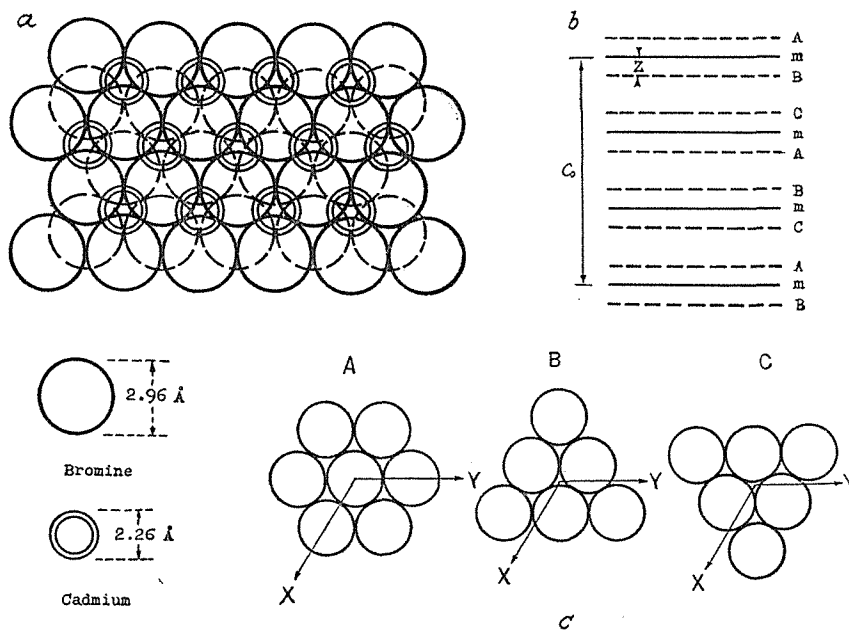


Fig. 2. The lattice structure and the stacking manner of atoms in cadmium bromide crystal.

of this type has a layered structure composed of hexagonally close-packed double sheets of halogen ions with the small metallic cations in the interstices of this packing as shown in Fig. (2). The lateral stacking manner of neighbouring sheets becomes (AmB) (CmA) (BmC) (AmB)...., where A, B and C are the three possible positions of a hexagonally close-packed sheet in the lateral direction, as shown in Fig. 2 (b) and (c), and is well known as the rhombohedral stacking<sup>8)</sup>.

For cadmium bromide, which has the above crystal structure, the unit cell constants are given to be  $a_0 = 3.954 \text{ \AA}$ ,  $c_0 = 18.672 \text{ \AA}$ , and  $V = 252.8 \text{ \AA}^3$  in the hexagonal description in place of the rhombohedral one for convenience of calculation. The atomic positions are given as follows<sup>9)</sup> :

$$\begin{aligned} \text{Cd} : & 000; \quad 1/3, \quad 2/3, \quad 1/3; \quad 2/3, \quad 1/3, \quad 2/3, \\ \text{Br} : & 00u; \quad 00u; \quad 1/3, \quad 2/3, \quad u+1/3; \quad 1/3, \quad 2/3, \quad 1/3-u; \\ & 2/3, \quad 1/3, \quad u+2/3; \quad 2/3, \quad 1/3, \quad 2/3-u, \end{aligned}$$

where  $u$  is the unknown parameter and requires the precise determination in the present work.

Taking extinction law given for this stacking,  $h + k - l = 3n$ , into account, the structure factor  $F_{hkl}$  can be easily simplified with the data of atomic positions as follows:

$$F_{hkl} = 3(Z_R - f_R) + 6(Z_X - f_X) \cdot \cos 2\pi ul, \quad (11)$$

where  $Z$  and  $f$  are atomic number and the atomic scattering factor for X-ray respectively and the suffixes R and X correspond to cadmium and bromine. Thus  $V_{hkl}$  is finally given as follow:

$$V_{hkl} = 0,054 d_{hkl}^2 [(Z-f)_{Ca}^2 + 2(Z-f)_{Br} \cos 2\pi ul], \quad (12)$$

In practice, the  $u$  value can be determined by the use of the  $V_{hkl}$  curves for various  $hkl$  planes previously drawn against the parameter  $u$  and by taking the experimentally obtained  $V_{hkl}$  values on the curves.

### III. EXPERIMENTAL

#### i) Apparatus

The electron diffraction unit used here is the three-stage electron microscope, SM-C3 which has the specimen holder for electron diffraction of high resolution work at the position between the intermediate and projector lenses. The image of the cross-over point of the electron source is reduced in size by objective lens and the intermediate lens projects it on the screen. Thus, the high resolution type electron diffraction pattern can easily be obtained. The projector lens, when operated in coordination with the intermediate one, can project the magnified shadow image of the specimen on the screen in place of the diffraction pattern of the same part. This can be used to detect the aspect of the crystal from which the diffraction pattern is originated. The intermediate diaphragm, whose aperture size can be continuously changed, was used to limit the area of the specimen as small as possible to avoid the confusion by the stray diffraction spots coming from unaimed crystals and any other disturbance of the subsidiary maxima from unexpected causes such as the simultaneous reflections within the

crystal itself. Close attention was also paid to avoid the specimen change under the electron irradiation, as the sublimating point of cadmium bromide is rather low. The exposure was therefore limited within a range from 30 seconds to 2 minutes. By such precautions, no change can be observed either on the diffraction pattern or in the electron image of the specimen at all.

### ii) Specimen

The micro-crystal of cadmium bromide were prepared and mounted on the specimen trager by the sublimation method in dried carbon dioxide to avoid the effect of water and oxidation in recrystallization. The electron diffraction pattern for each crystal proved that the micro-crystals are cadmium bromide of rhombohedral stacking. In this case, chemically prepared pure micro-crystals of gold<sup>10</sup> were used as the reference for the precise analysis of the spacings.

Some examples of the electron shadow images of the crystal are shown in Fig. 3 together with the electron diffraction pattern corresponding to each crystal, by which the identification was made. The azimuthal orientation of the two pattern was corrected for each pair. The size of the crystal is distributed over a range from about 2 to 10 microns in the width of the hexagonal flat surface, and the thickness is about a few hundred angstroms. The shape of the crystal is nearly hexagonal with round apices. Sometimes it rolled itself to a tube as in Fig. 3 (e'). In such a case, the diffraction pattern becomes very complex accompanied by the double diffraction and the simultaneous reflection. In another case, not so extreme as in (e'), the crystals have more or less fortuitous warping which can be proved, as Heidenreich<sup>11</sup> pointed out, by the parallel extinction fringes appearing on the habit surface, which were caused by the reflection of

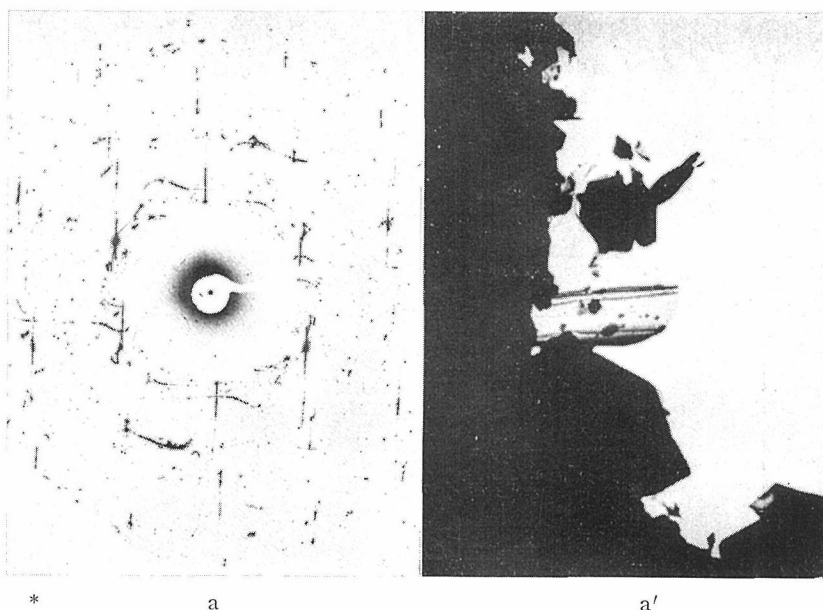
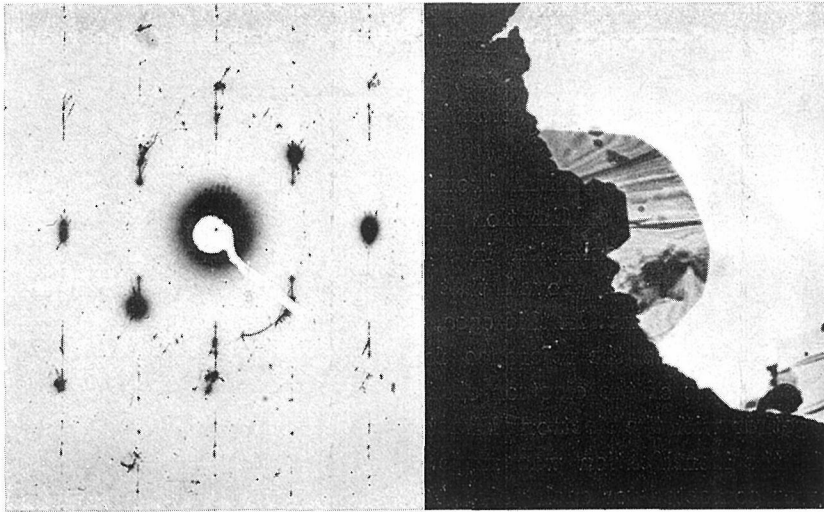
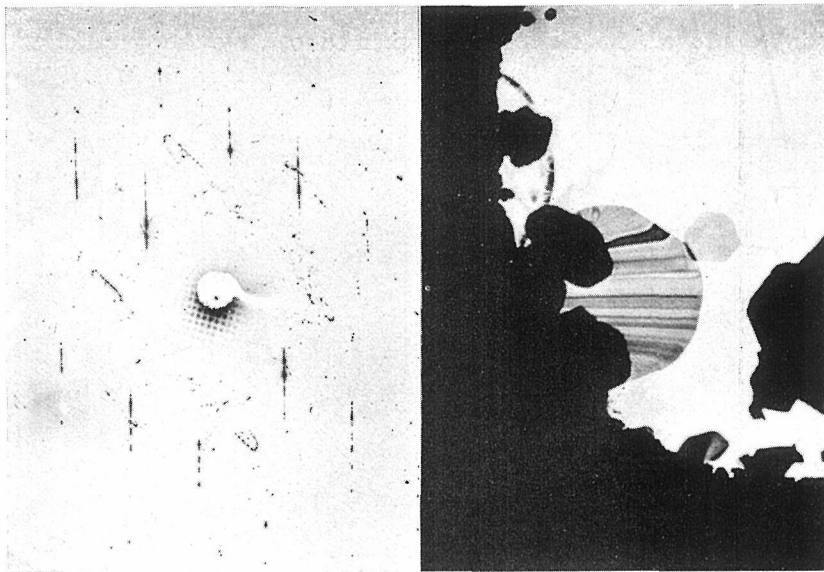


Fig. 3. The electron shadow micrographs of lamellar single micro-crystal of cadmium bromide and their electron diffraction patterns.



b

b'



c

c'

Fig. 3. Continued.

Crystal Structure Analysis by Subsidiary Diffraction Maxima

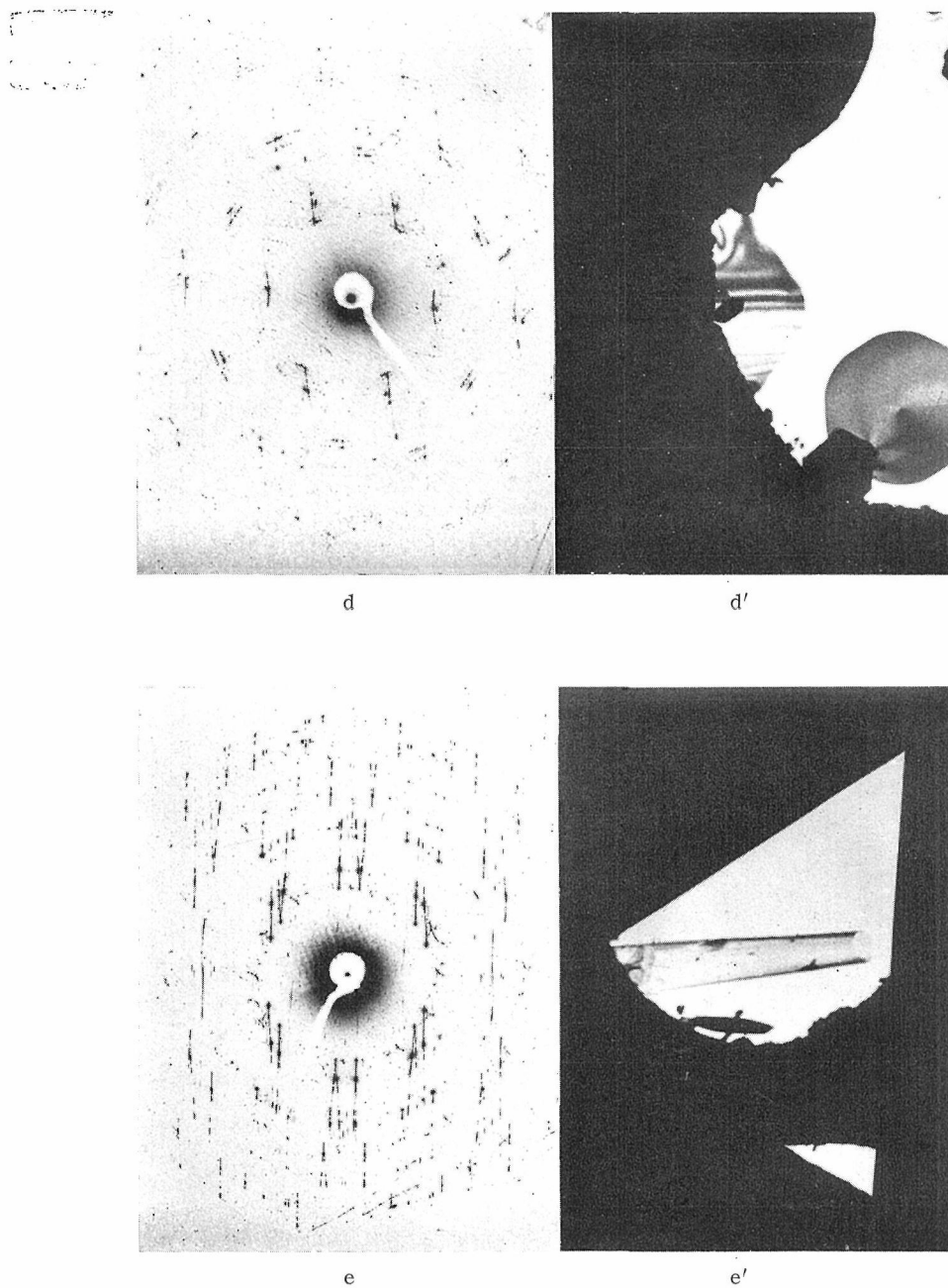


Fig. 3. Continued.

Natsu UYEDA

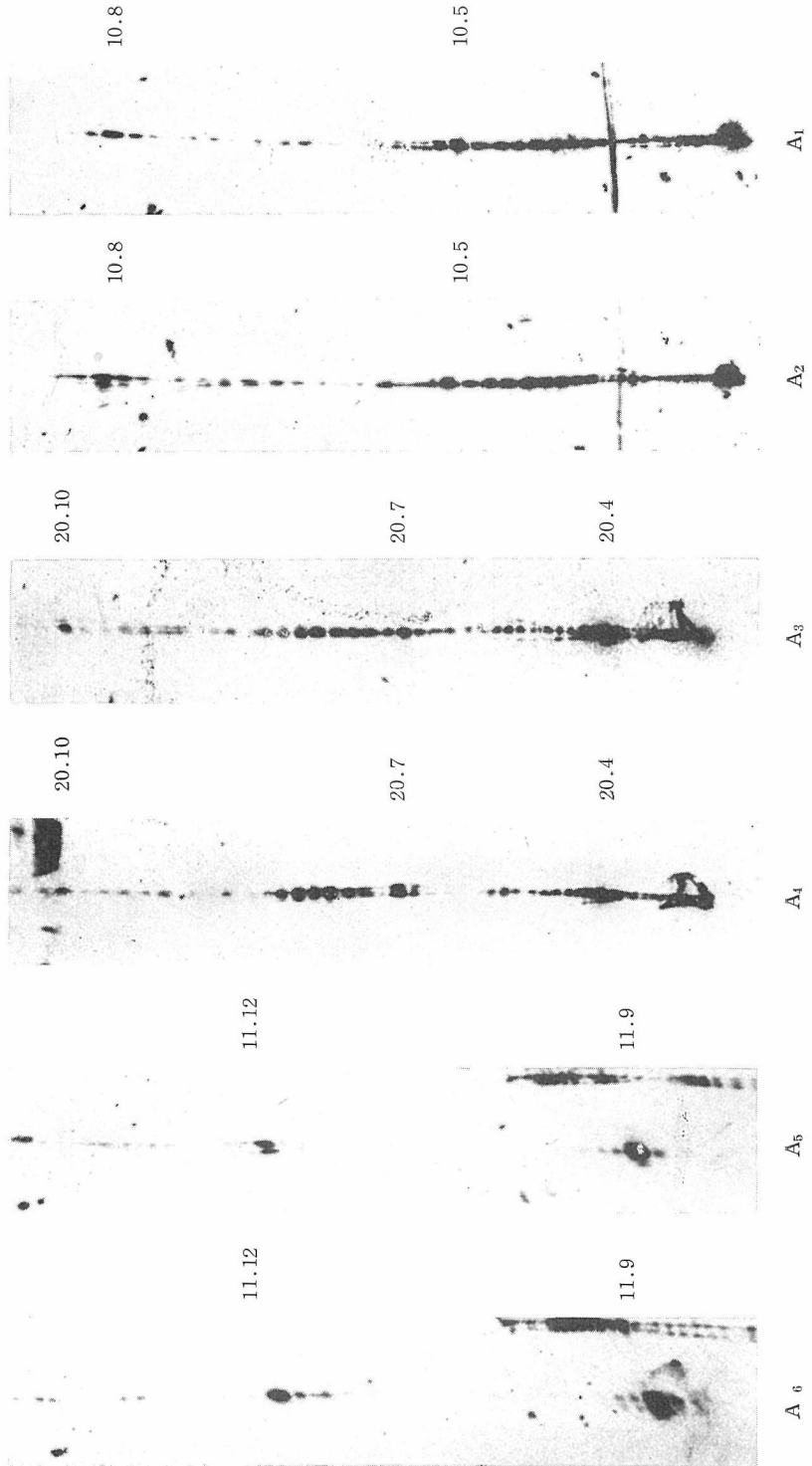


Fig. 4. Magnified photographs of elongated diffraction spots containing the subsidiary maxima.

Crystal Structure Analysis by Subsidiary Diffraction Maxima

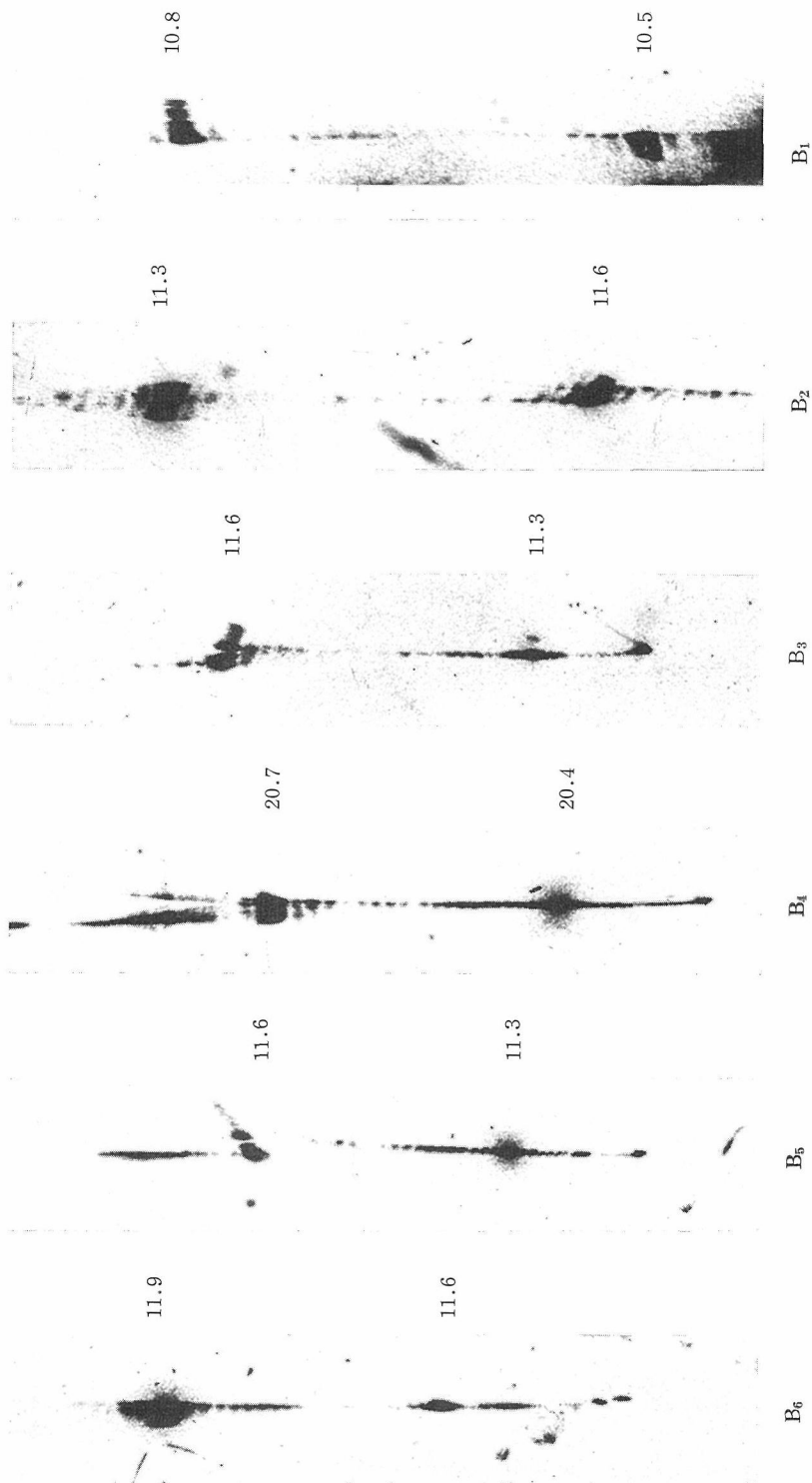
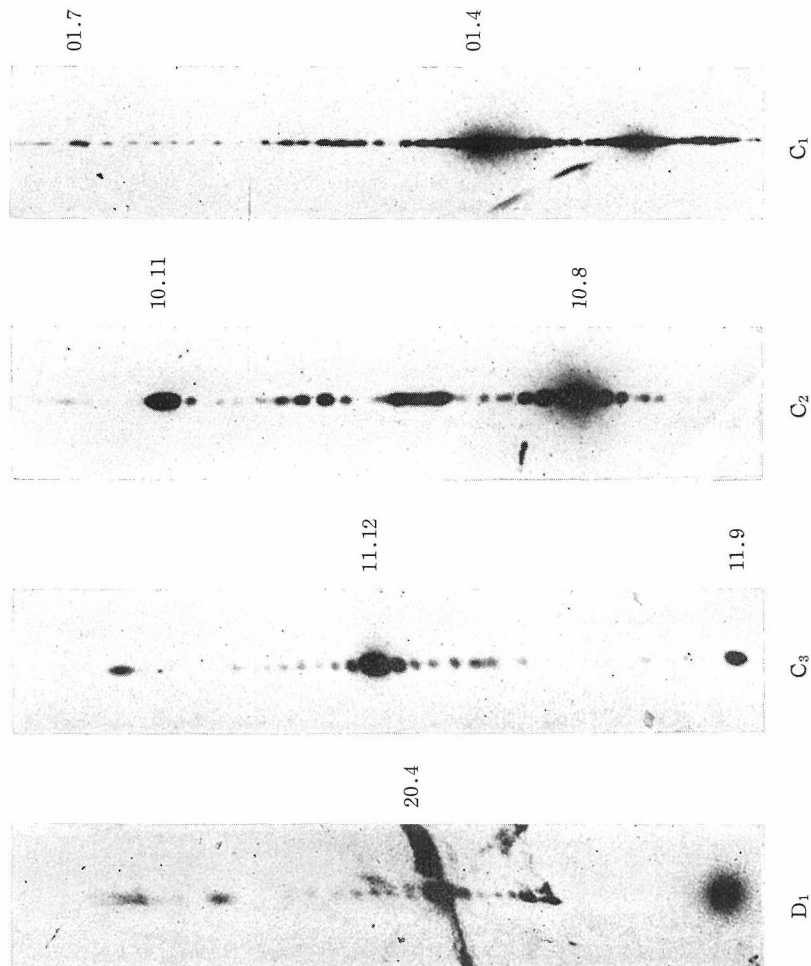


Fig. 4. Continued.



electron at the part of the crystal where the inclination makes for suitable lattice planes to fulfil the Bragg condition.

#### IV. RESULTS AND DISCUSSION

The electron diffraction pattern shown in Fig. 3 has the parallel elongations of diffraction spots in the direction normal to the extinction fringes of the corresponding electron image of the crystal. The subsidiary maxima ranking in those elongations are distinctly detectable in the magnified photographs collected in Fig. 4. Effective camera length was also extended to about 8 to 10 meters. The precise final magnification of the photographs was determined from the distance between the main diffraction spots. With those photographs, the displacement  $\Delta r_n$  of each subsidiary diffraction spots from the principal one was measured by the distance between the centers of each spots and the angular displacement  $\Delta\theta_n$  was calculated. The set of the  $h_n$  values are calculated using the  $\Delta\theta_n$  values thus obtained through Eq. 6. The value of  $\theta_1$  was obtained by taking the orientation of the crystal to incident beam into account. The wave length  $\lambda$  can be

Crystal Structure Analysis by Subsidiary Diffraction Maxima

precisely determined with diffraction pattern itself using the accurate camera length of the apparatus.

On the other hand, as a linear relationship exists in Eq. 4 between  $h_n^2$  and  $(n + 1/2)^2$ , the value of M can be estimated from the inclination of the line. M is generally an integer for a crystal, then the nearest integer value must be assigned to it, as the initial M obtained from the inclination is not always an integer. With the value of M thus modified the  $h_n$  value can also be corrected through the same linear relationship. Using those  $h_n$  value,  $V_{hkl}$  was calculated as shown in

Table 1. Geometrical quantities of electron diffraction pattern, Fourier potential  $V_{hkl}$  and parameter u for CdBr<sub>2</sub>.

<i>hkl</i>	<i>d</i> (Å)	<i>n</i> =1	2	3	4	$\mu$	$\theta_1$	$\theta_2$	$\gamma$	$\lambda$ (Å)	$E$ (kV)	$V_{hkl}$ (eV)	<i>u</i>
A 10.5	2.524	0.3951 0.0610	0.7088 0.1032	0.9598 0.1452		47°28'	44°	45°17'	3°20'	0.0587	41.88	3.8	0.247
10.8	1.928	0.3595 0.0498	0.7953 0.1001			34°25'	57°	58°42'	2°	//	//	6.9	0.244
11.9	1.431	0.4554 0.0619	0.7919 0.1037	1.0709 0.1455		46°43'	47°30'	49°40'	30°	//	//	2.5	0.248
11.12	1.222	0.4900 0.0602	0.8550 0.1028	1.577 0.1449		38°11'	49°	51°12'	24°30'	//	//	4.2	0.246
B 10.5	2.524	0.4711 0.0702	0.8462 0.1183	1.1649 0.1663		47°28'	44°	45°43'	22°20'	0.0592	41.15	3.6	0.248
10.8	1.928	0.5038 0.0632	0.0015 0.1141	1.4499 0.1631		34°25'	57°	58°42'	22°20'	//	//	6.9	0.245
11.3	1.884	0.2993 0.0712	0.4213 0.1189	0.6036 0.1667	0.8863 0.2141	72°25'	20°	21°32'	30°	//	//	2.6	0.249
20.4	1.608	0.2320 0.0659	0.4139 0.1179	0.5792 0.1658	0.7504 0.2137	69°53'	20°	21°59'	0°	//	//	5.9	0.245
20.7	1.441	0.3656 0.0707	0.6285 0.1186	0.8791 0.1664	1.1584 0.2141	57°19'	34°20'	36°28'	0°	//	//	3.1	0.249
11.9	1.431	0.4970 0.0708	0.8400 0.1187	1.1421 0.1664		46°43'	47°30'	49°42'	21°	//	//	2.4	0.248
C 01.4	2.761	0.5962 0.0853	1.0556 0.1403	1.2902 0.1811		53°29'	58°	59°12'	44°	0.0540	49.10	9.8	0.242
01.7	2.104	0.4104 0.0594	0.7695 0.1025	1.1824 0.1447	1.4902 0.1868	38° 0'	70°	71°17'	31°30'	//	//	2.4	0.248
10.8	1.928	0.3812 0.0542	0.7259 0.0979	1.0594 0.1436	1.4013 0.1854	47°28'	57°30'	59° 4'	6°30'	//	//	7.0	0.246
10.11	1.521	0.4052 0.0618	0.7479 0.1038			60°54'	64°30'	66°33'	5°	//	//	1.6	0.247
11.9	1.431	0.3699 0.0612	0.6492 0.1036	0.9021 0.1455	1.2985 0.1873	46°43'	48°	50° 4'	16°	//	//	2.6	0.247
11.12	1.222	0.7821 0.1030	1.0738 0.1446	1.3920 0.1863	1.5996 0.2290	38°11'	51°	59°28'	14°	//	//	4.2	0.245
D 20.4	1.608	0.5264 0.1493	0.8592 0.2493	1.2532 0.3497	1.6471 0.4497	70°	20°	24°44'	19°	0.0546	48.20	5.9	0.241

Table 2. Calculated  $V_{hkl}$  values for varying parameter, expressed in unit of eV.

$hkl$	$d(\text{\AA})$	$u$ 0.23	0.24	0.52	0.26	0.27
01.4	2.761	9.1	9.7	9.9	9.7	9.1
10.5	2.524	6.6	5.0	3.3	1.6	0.0
01.7	2.104	-0.79	0.9	2.9	4.9	6.6
10.8	1.928	5.0	6.6	7.1	6.6	5.0
11.3	1.884	1.1	1.9	2.7	3.5	4.3
20.4	1.608	5.5	5.8	6.0	5.8	5.5
10.11	1.521	-1.2	-0.1	2.1	4.3	5.4
20.7	1.441	-0.83	1.2	3.6	6.1	8.1
11.9	1.431	5.0	3.8	2.0	0.3	-0.9
11.12	1.222	1.9	3.6	4.4	3.6	1.9

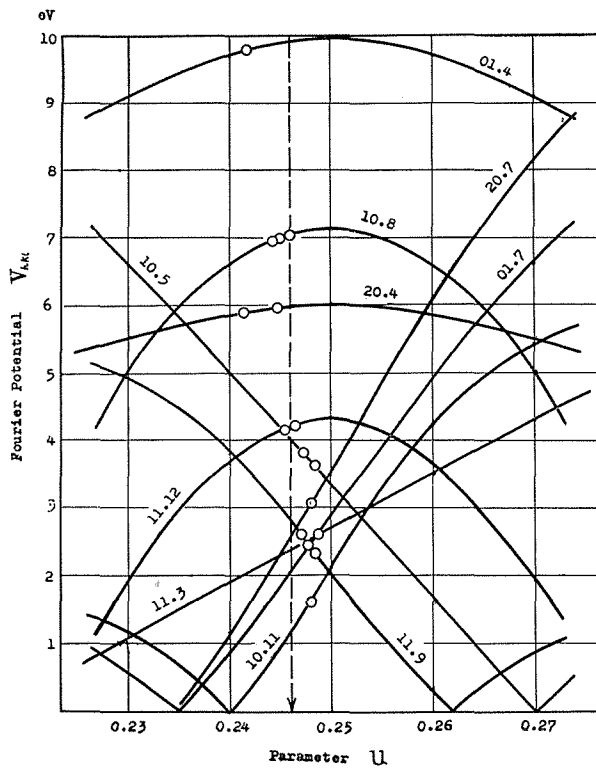


Fig. 5. Fourier potential *versus* parameter curves of CdBr<sub>2</sub>.

Table 1, again through Eq. 4, where  $E$  was determined using the wave length  $\lambda$  and  $\theta_1$  is the same with the one used in Eq. 6. The value of  $\theta_2$  was estimated by taking the Bragg angle  $\theta_R$  of the  $(hkl)$  reflection and the angle  $\mu$  between the normals of the habit surface and the  $(hkl)$  plane, through Eq. 12:

$$\cos\theta_2 = \cos 2\theta_B \cdot \cos \theta_1 - \sin 2\theta_B \cdot \cos\mu, \quad (12)$$

The values for  $h_n$ ,  $\theta_1$  and  $\theta_2$  are also given in the same table.

On the other hand  $V_{hkl}$  value was calculated for various  $(hkl)$  indices, in the range of  $u$  from 0.23 to 0.27, as shown in Table 2. In Fig. 5,  $V_{hkl}$  versus  $u$  curves are collected for the same range. The curve has its maxima at  $u = 0.25$  and becomes symmetrical on both sides of this point for the reflection whose  $l$  is even, while for the reflection whose  $l$  is odd, the curve becomes asymmetrical. As in the above method no information can be obtained about the sign of the Fourier potential from the experimental value, the curve is always constructed by the absolute  $V_{hkl}$  value, i. e.  $|V_{hkl}|$ . On these curves, experimentally obtained  $V_{hkl}$  values were taken from the axis of ordinates as shown in the figure. The  $u$  value obtained from reflection is also shown in Table 1 and falls near a value about 0.25 though some deviations exist. Ideally, these values should become constant and points lie on a line vertical to the axis of abscissas. The averaged value of  $u$  in the present case becomes  $0.246 \pm 0.002$ , and is shown by the vertical broken line in the figure. For the parameter curve, whose index has even  $l$  and the maxima at  $u = 0.25$ , two  $u$  values can be obtained for one  $V_{hkl}$  value. In such a case, the more suitable value of the two must be selected, taking into account the  $u$  value which can be determined with the curve whose index has odd  $l$ . The value thus obtained for cadmium bromide is a reasonable one when compared with those for metallic halide crystals which have the layered structure of the same space group such as  $\text{CdCl}_2$  ( $u = 0.25$ ),  $\text{CoCl}_2$  ( $u = 0.25$ ),  $\text{NiBr}_2$  ( $u = 0.255$ ),  $\text{NiI}_2$  ( $u = 0.25$ ).

The accuracy of this method mainly depends on the measurement of  $\Delta y_n$ , the displacement of the subsidiary diffraction maxima. For precise measurement, it is effective to take successively two or three photographs of the diffraction pattern under the same condition but varying the exposure time, as is often carried out in the case of the intensity measurement. The position of the subsidiary maxima nearer the main one can be precisely determined with the less exposed plate and that of more distant ones with the more exposed plate. The value of  $V_{hkl}$  would be obtained within an error of about 5% as suggested from the results so far obtained by many workers with the crystal of known structure. The accuracy to determine the parameter graphically from the  $V_{hkl}$  value as in the present work varies with the shape of the parameter curve, which depends on the index of the reflection. For such suitable reflection as (20.7), (01.7), etc., even an error of 10% in the  $V_{hkl}$  value causes only 1–2% in  $u$  value. Therefore, if the  $V_{hkl}$  value is precisely determined, a comparatively accurate value of parameter would be obtained.

For more precise determination of the parameter, the effect of thermal vibration of each atom in the lattice plane must be taken into consideration for the construction of the parameter curve. In the case of cadmium bromide, the anisotropic vibration of the atoms, caused by the layered structure, makes the matter more complex. As this is the first report on the new method of determining the crystal parameter, based entirely on the geometrical quantity only, the more precise determination of the parameter will be left for further investi-

gations.

### ACKNOWLEDGMENT

The author would like to express his sincere thanks to Dr. K. Tanaka, Kyoto University, and Dr. H. Hashimoto, Kyoto Technical University for their helpful advice and discussion, and also to Dr. R. Uyeda, Nagoya University, for his useful suggestion, and to Dr. Cowley, Commonwealth Scientific and Industrial Research Organization, Australia for his kind criticism. He would also like to express his sincere thanks to Dr. E. Suito, Kyoto University for his helpful encouragement.

### REFERENCES

- (1) H. A. Bethe, *Ann. Phys.*, **87**, 55 (1928).
- (2) MacGillavry, *Physica*, **7**, 333 (1940).
- (3) N. Kato and R. Uyeda, *Acta Cryst.*, **4**, 229 (1951).
- (4) J. M. Cowley, P. Goodman and A. L. G. Rees, *ibid.*, **10**, 19 (1957).
- (5) H. Hashimoto ; *J. Phys. Soc. Japan*, **9**, 150 (1954).
- (6) R. Uyeda, T. Ichinokawa and Fukano, *Acta Cryst.*, **7**, 216 (1954).
- (7) E. Suito and N. Uyeda, *Proc. Japan Acad.*, **19**, 331 (1953).
- (8) Z. Pinsker, "Electron Diffraction" Butterworth Sci. Publ., London (1953) p. 267.
- (9) R. W. G. Wyckoff, "Crystal Structure," I (1951) Interscience Publ., Inc., New York.
- (10) E. Suito and N. Uyeda, *J. Electronmicrosc.*, **1**, 33 (1953).
- (11) R. Heidenreich, *J. App. Phys.*, **20**, 993 (1949).

### APPENDIX

In the treatment described hereunder, the Ewald sphere is approximated by a plane passing through the origin as in the ordinary electron diffraction. The rotation axis of the reciprocal lattice caused by the bending of the crystal, in

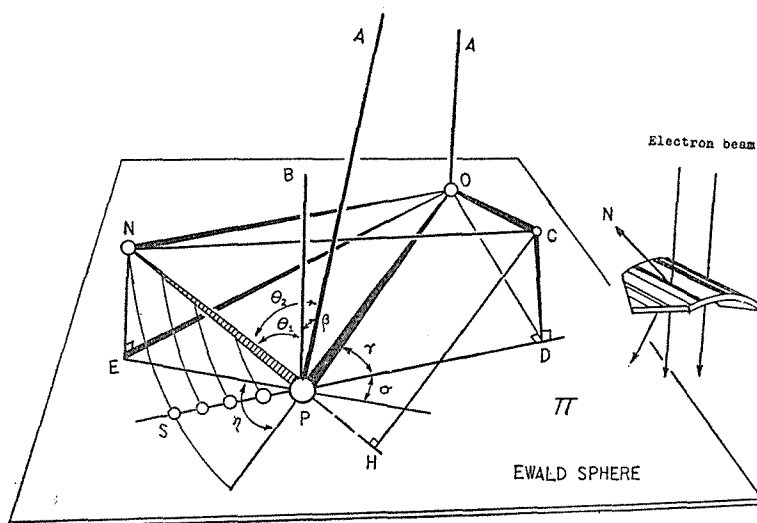


Fig. 6. Schematic illustration of the rotation of the reciprocal lattice for the arbitrarily warping crystal.



can be elucidated in the following simple relation, which can easily be found among the geometrical quantities as shown in Fig. 7 :

$$CN^2 = NK^2 + (CP + PK)^2 = CS^2 = (SP + PD)^2 + CD^2 = (SP + PD)^2 + (CP^2 - PD^2),$$

These equation can be rewritten in the following form where  $b' = PD$  :

$$z^2 = x_n^2 \cos^2 \theta + (x_n \sin \theta + y)^2 = (a_n + b')^2 + h_n^2 = (a_n + b')^2 + (y^2 - b'^2)$$

By simplification, an equation relating to the unknown quantity  $x_n$  can be obtained as follows :

$$x_n^2 + 2x_n y \cdot \sin \theta - (a_n^2 + 2a_n b') = 0. \quad (11)$$

By solving the equation with respect to  $x_n$ ,

$$x_n = (y^2 \sin^2 \theta + 2a_n y + a_n^2) - y \cdot \sin \theta, \quad (14)$$

which can again be rewritten by the use of the essential value which is defined in relation to the reciprocal lattice, such as

$$x_n = h_n / d_n, y \cdot \sin \theta = \cos \mu / d, a_n = \Delta \theta_n / \lambda, b' = \cos \gamma / d ; \quad (15)$$

When the angle  $\gamma$  is put equal to  $(\gamma + \sigma)$ , where  $\sigma$  represents  $\angle EPS$ , the following relationship exists as :

$$NP \cdot \sin \theta_1 \cdot \cos \gamma = EP \cdot \cos \gamma = NP \cdot \cos \mu,$$

and this proves the relationship as :

$$\sin \theta_1 \cdot \cos (\gamma + \sigma) = \cos \mu. \quad (16)$$

Therefore, Eq. 15 can be modified to the following form as :

$$h_n = d_N \left\{ \left\{ \frac{\sin^2 \theta_1 \cos^2 (\gamma + \sigma)}{d^2} + \frac{2 \Delta \theta_n \cos \gamma}{\lambda d} + \frac{\Delta \theta_n^2}{\lambda^2} \right\}^{\frac{1}{2}} - \frac{\sin \theta_1 \cos (\gamma + \sigma)}{d} \right\} \quad (17)$$

Furthermore, by replacing  $\Delta \theta_n / \lambda$  with  $\Delta r_n / (r d)$ , the following equation can be derived from Eq. 15 as :

$$h_n = \frac{d_N}{d} \left\{ \left\{ \cos^2 \mu + 2 \frac{\Delta r_n}{r} \cos \gamma + \left( \frac{\Delta r_n}{r} \right)^2 \right\}^{\frac{1}{2}} - \cos \mu \right\} \quad (18)$$

Where the third term in the parenthesis may often be neglected as it becomes a very small quantity. And in the case, where the rotation axis is contained in the Ewald sphere,  $\sigma$  vanishes, and Eq. 18 results:

$$h_n = \frac{d_N}{d} \left\{ \left\{ \sin^2 \theta_1 \cos^2 \gamma + 2 \frac{\Delta r_n}{r} \cos \gamma + \left( \frac{\Delta r_n}{r} \right)^2 \right\}^{\frac{1}{2}} - \sin \theta_1 \cos \gamma \right\} \quad (19)$$

This is the most convenient equation for practical calculation of  $h_n$  value from the diffraction data.